TISSUE ENGINEERING: Part A
Volume 21, Numbers 9 and 10, 2015
DOI: 10.1089/ten.tea.2014.0477

Pushing the Envelope in Tissue Engineering: *Ex Vivo* Production of Thick Vascularized Cardiac Extracellular Matrix Constructs

Udi Sarig, PhD,[1,2,*] Evelyne Bao-Vi Nguyen, MSc,[2,*] Yao Wang, MSc,[2] Sherwin Ting, BSc,[3] Tomer Bronshtein, PhD,[1] Hadar Sarig, PhD,[2] Nitsan Dahan, PhD,[1] Maskit Gvirtz, MSc,[1] Shaul Reuveny, PhD,[3] Steve K.W. Oh, PhD,[3] Thomas Scheper, PhD,[4] Yin Chiang Freddy Boey, PhD,[2] Subbu S. Venkatraman, PhD,[2] and Marcelle Machluf, PhD[1,2]

Functional vascularization is a prerequisite for cardiac tissue engineering of constructs with physiological thicknesses. We previously reported the successful preservation of main vascular conduits in isolated thick acellular porcine cardiac ventricular ECM (pcECM). We now unveil this scaffold's potential in supporting human cardiomyocytes and promoting new blood vessel development *ex vivo*, providing long-term cell support in the construct bulk. A custom-designed perfusion bioreactor was developed to remodel such vascularization *ex vivo*, demonstrating, for the first time, functional angiogenesis *in vitro* with various stages of vessel maturation supporting up to 1.7 mm thick constructs. A robust methodology was developed to assess the pcECM maximal cell capacity, which resembled the human heart cell density. Taken together these results demonstrate feasibility of producing physiological-like constructs such as the thick pcECM suggested here as a prospective treatment for end-stage heart failure. Methodologies reported herein may also benefit other tissues, offering a valuable *in vitro* setting for ''thick-tissue'' engineering strategies toward large animal *in vivo* studies.

Introduction

Despite major advancements in the fields of biomaterials and cell biology, limited success has been reported in cardiac regeneration following myocardial infarction, regardless of the material type or cell delivery platform used (i.e., patch or injection based).[1–3] The clinical application of existing solutions is limited by the lack of functional vascularization,[4–6] the inability to ensure efficient cell support in clinically relevant thick tissue constructs[7,8] and the availability of scaffold biomaterials matching the mechanical and biochemical properties of the myocardium.[1,9]

Vascularization is particularly important in constructs exceeding the thickness of 100–150 μm, representing the diffusion limitation of soft tissues under static culture conditions.[1,7,10–14] Moreover, the ultimate thicknesses achieved under dynamic culture conditions (< 600 μm), are still far from that of the natural left ventricular wall (~10–15 mm).[1]

Consequently, however encouraging the data published to date may be, the lack of a connectable vascular tree during transplantation has led to a long lag time while angiogenesis occurs, speculated to result in minimal cell retention in the heart's harsh environment. Vascularization is needed both to support the establishment of *ex vivo* cultivated cell-seeded constructs,[1,4–7,15] and to provide a connectable vascular tree that can instantly supply the tissue upon transplantation. Hence, the development of dynamic culture methodologies enabling the production of clinically relevant tissue-engineered constructs with a connectable vascular network will have clear implications for this field and is needed to advance this platform toward clinical application.

[1]The Laboratory of Cancer Drug Delivery & Mammalian Cell Technology, Faculty of Biotechnology and Food Engineering, Technion–Israel Institute of Technology, Haifa, Israel.
[2]School of Materials Science and Engineering, Nanyang Technological University, Singapore.
[3]Bioprocessing Technology Institute, Agency for Science Technology and Research (A*STAR), Singapore.
[4]Institute of Technical Chemistry, Leibniz University, Hanover, Germany.
*These two authors contributed equally to this article.

© Udi Sarig *et al.* 2015; Published by Mary Ann Liebert, Inc. This Open Access article is distributed under the terms of the Creative Commons Attribution Noncommercial License (http://creativecommons.org/licenses/by-nc/4.0/) which permits any noncommercial use, distribution, and reproduction in any medium, provided the original author(s) and the source are credited.

Recently, our group and others described the isolation of cardiac acellular extracellular matrix (ECM) from rats[16,17] and pigs,[7,18–23] which was proposed as an ideal scaffolding biomaterial for cardiac regeneration. The decellularization of full-thickness porcine cardiac ventricular ECM (pcECM) is potentially advantageous, over other tissues and species, as it highly resembles the human ventricular wall in structure, size, and composition.[24,25] In this study we aimed to strengthen our ability to support such a platform, demonstrate the potential of this thick pcECM scaffold, and evaluate its long-term cell support and the *ex vivo* promotion of new blood vessel generation. For these purposes, a unique bioreactor system was designed and custom built, enabling the long-term compartmentalized cocultivation of various stem and progenitor cells within the thick pcECM construct under dynamic physiological-like conditions. Cocultures of human umbilical vein endothelial cells (HUVECs) and human mesenchymal stem cells (hMSCs) were used herein as a proof-of-concept to demonstrate the inherent vasculature functionality and its ability to support the *ex vivo* repopulation of the thick tissue construct's bulk. Furthermore, a simple methodology was developed to statically determine the pcECM cell holding capacity, predicting a maximal cell density resembling that of native myocardium. Taken together, our study demonstrates for the first time the possibility of reconstructing a *functional* vascular tree *ex vivo*, which supports compartmentalized recellularization of thick myocardial-like tissue constructs. Our study suggests an alternative and important approach to cardiac tissue engineering, which is based on preserving a connectable *inherent* vascular tree within the biomaterial scaffold that might facilitate future survival and function of reseeded constructs upon transplantation.

Materials and Methods

Preparation of pcECM matrices for static and dynamic culturing

Porcine left ventricular full-thickness slabs ($\sim$10–15 mm) were perfused and decellularized as previously described.[7] For static cultivation, thick pcECM matrices were placed on standard culture plates and cut with a sterile 8 mm punch (unless stated differently). Matrices were transferred into 96-well plates, epicardial surface facing downwards. For dynamic cultivation, pcECM matrices were cut using a scalpel into $\sim 25 \times 75 \times 15$ mm slabs containing the perfusion entry catheter already sutured in place (24-gauge, 8 cm long; Biometrix™). Ethanol disinfected catheters (20 min in 70% ethanol) were sutured using a sterile suturing thread (5/0 nonabsorbable thread) to the other side of the lateral anterior descending coronary artery for drainage. Large leaks, if detected, were shunted by additional suturing. Before cell seeding, matrices of either cultivation method were washed with ethanol 70% (1×30 min, 1×2 and 1×12 h) followed by at least three washes with phosphate-buffered saline (PBS; 3×30 min), immersion in complete culture media for 12 h, and air-drying in a sterile hood for 2 h.

Cell isolation and cultivation

Bone marrow hMSCs were purchased from Lonza and cultured in humidified incubator at 37°C and 5% CO_2 using alpha modified Eagle's medium (α-MEM; Biological Industries) supplemented with 20% fetal bovine serum, 1% Pen-Strep, and 0.4% Fungizone®. HUVECs stably expressing GFP (HUVEC-GFP) were kindly donated by Prof. Gera Neufeld (Technion, Faculty of Medicine)[26] and cultured on gelatin-coated plates (0.2% gelatin in PBS, 37°C, >4 h; Sigma-Aldrich™) with M199 culture media supplemented with 20% fetal calf serum, 1% Pen-Strep®, and 0.4% Fungizone (Life Technologies). Basic fibroblast growth factor (10 ng/mL) was added to plates of both cell types every other day. Whenever HUVECs and hMSCs were cocultured, α-MEM was used. Human embryonic stem cell-derived cardiomyocytes (hESC-CM) were expanded, differentiated, and statically cultivated on the pcECM following protocols described in Supplementary Methods (SM) section 1.5 (Supplementary Data are available online at www.liebertpub.com/tea).

Assessment of pcECM cell support

To evaluate the pcECM maximal cell capacity under static culture conditions, mathematical modeling was employed as detailed in the SM section 1.2. This model was based on empirical data and verified by an additional set of experiments in which the quantity of cell adhesion foci was artificially changed, for example, through cross-linking of hyaluronic acid (HA) to the pcECM matrices, to investigate the model sensitivity. Detailed information about the model development, various screening experiments for adhesion site modifications, and the model verification studies is presented in the SM sections 1.1–1.3.

The static seeding and cultivation of hMSCs on the pcECM scaffolds for the mathematical modeling were performed according to our previously published procedure with slight modifications.[7] Briefly, pcECM scaffolds (8 mm in diameter) were immersed in 96-well plates containing α-MEM complete culture media for 12 h in cell-culture conditions. Before seeding, media was removed and scaffolds were left to partially dry for 2 h. HMSCs were resuspended in complete α-MEM, to a final concentration of 1.4×10^4 cells/μL, seeded on the matrices with increasing cell densities (5×10^4, 2×10^5, 4×10^5, and 1.5×10^7 cells/cm^2 in quintuplicate per each density), and cultivated for 21 days. Seeding was performed through pipettation by slowly administering the appropriate cell suspension volume (as per the cell quantities detailed above) onto the center of the scaffolds. Seeded scaffolds were preincubated in culturing conditions for 90 min, previously reported by us as the optimal seeding time,[7] and transferred to new plates for cultivation. Unless mentioned otherwise, each reseeded matrix was incubated in 2 mL of hMSC complete growth media, replenished every other day. Similar experiments were also performed with HUVECs as detailed in the SM section 1.2.

Bioreactor system design and setup

A schematic description of the bioreactor design and setup used throughout these experiments is presented in Figure 1. The ''heart'' of the system is the perfusion chamber (Fig. 1a-5–c). This custom-built chamber holds the matrices in place (marked by a red mesh in Fig. 1c) under sterile culture conditions, and it enables both pulsatile flow perfusion and future mechanical and electrical stimulation,

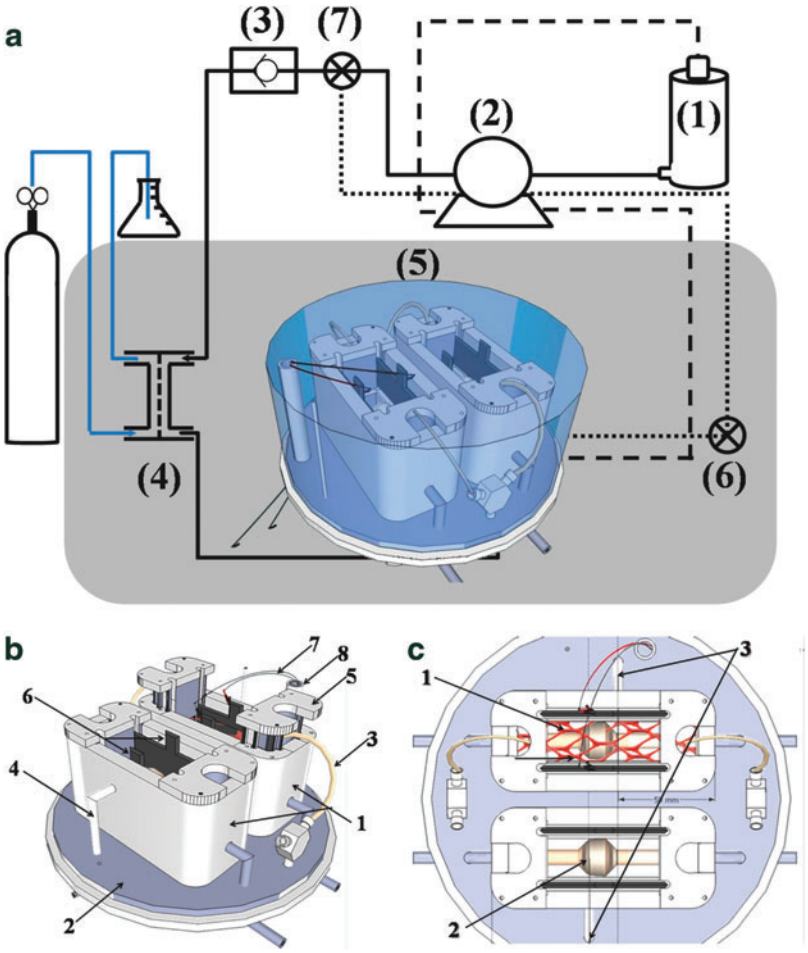

FIG. 1. A custom-designed bioreactor system. An overview of the system components **(a)**, showing a medium reservoir **(1)**, which supplies culture media through a peristaltic pump **(2)**, a check valve **(3)** and an oxygenator **(4)** to a perfusion chamber **(5)**. Two separate lines are responsible for drainage either back to the reservoir (*dashed line*) or using a smaller volume cycle for cell quantifications (*dotted line*). *Gray* shade represents a standard CO_2 incubator. **(6, 7)** Represent three-way faucets and sampling ports. The perfusion chamber **(b, c)** has two identical perfusion baths **(b-1)** for statistical repetition, which are located on an elevated base plate through which all tubing connections are passed **(b-2)**. The baths are drained from the side using the low volume cycle **(b-4, c-3)**. The thick porcine cardiac ventricular ECM matrix (marked by a *red* mesh in **c-1)** is fed by a 24-gauge silicon catheter **(b-3)** and is held in place by two holders **(b-5)**. A balloon **(c-2)** and electrode **(b-6, b-7,** and **b-8)** subsystems will enable future mechanical and electrical stimulation, though these devices were not directly assessed herein. Color images available online at www.liebertpub.com/tea

mimicking the heart physiological environment. The glass cover enables online monitoring and imaging under sterile culture conditions. The chamber is located within a standard CO_2 incubator (marked by gray-shaded square in Fig. 1a), maintaining a temperature of 37°C throughout the system. A MasterFlex™ peristaltic pump (Fig. 1a-2) is used to pump the culture media from a glass medium reservoir (Fig. 1a-1; Radnoti LLC) to the perfusion chamber. A silicon tube oxygenator (Fig. 1a-4; Radnoti LLC) and a no-return check valve (Fig. 1a-3; Cole Parmer), located between the pump and the perfusion chamber ensure maintenance of proper oxygen levels. A second channel for drainage of excess culture media from the bioreactor (marked by a dashed line) pumps the media back into the reservoir. A third low-volume channel (dotted line) is used to bypass the reservoir when concentration-dependent measurements are taken to assess cell quantity and metabolic state throughout long-term experimentation. System installation, cell seeding, and standard operation procedure are detailed in the SM sections 1.6 and 1.7.

Determining the dynamic cultivation parameters

To determine the optimal seeding time and perfusion flow rate, acellular pcECM constructs were seeded with hMSCs (see SM section 1.7), installed in the perfusion chamber baths, covered with 60 mL of complete MSC culture media, and incubated for 1.5 or 24 h before starting perfusion, allowing cell attachment. To measure cell viability, 5% AlamarBlue™ (Invitrogen™) in complete culture media was perfused for 24 h (low volume cycle, bypassing the reservoir) at 40 or 80 mL/min. Media samples (300 µL) were taken throughout the culture via the sampling port (Fig. 1a-6), the AlamarBlue fluorescence intensities were measured (Ex: 530/25 nm, Em: 595/35 nm), and cell numbers were calculated thereof versus the appropriate calibration curve. The survival rate determined 24 h postcommencement of perfusion was estimated by dividing the AlamarBlue determined cell quantities with the initial seeding quantity (1.4×10^7 cells/construct). In another experiment, we assessed the optimized cultivation parameters (1.5 h seeding time, 120 mL/construct perfused at up to 40 mL/min and replenished every other day) in terms of hMSC support for up to 7 days (SM section 1.7). Constructs were cross sectioned and stained with hematoxylin and eosin (H&E). Representative images are presented out of a total of three constructs processed and at least three histological cross sections per construct.

Compartmentalized recellularization

The optimized dynamic cultivation parameters were further assessed in terms of their effect on constructs, which were precultivated in steady state densities under static culture conditions. Thus, hMSCs (3×10^5 cells/cm^2) were seeded onto the endocardial surface of $25 \times 70 \times 15$ mm

acellular pcECM slabs, statically monocultured for 30 days, and transferred to the bioreactor system for dynamic culturing for an additional period of 14 days. Cell viability (AlamarBlue), density and penetration toward the feeding blood vessels (histology) were assessed. Alternatively, HUVECs stably expressing GFP were resuspended (10×10^6 cells/mL) in 0.2% gelatin in complete M199 culture media and seeded through the vascular network. Fourteen days postseeding live imaging was performed through confocal microscopy to evaluate the extent of vascular network coating, followed by histological cross section and staining with CD31. More detailed information on the experimental methodology employed can be found in the SM section 1.8.

Dynamic cocultivation of re-endothelialized acellular pcECM

Long-term coculture of HUVEC-GFPs and MSCs was studied for 21 days. HUVEC-GFPs were seeded into the inherent vasculature of acellular pcECM slabs as we previously published[7,27] with slight modifications, detailed in the SM section 1.7 and Supplementary Figure S1. Re-endothelialized matrices ($n=3$) were mounted onto the perfusion chamber and incubated for 1.5 h before starting perfusion (up to 40 mL/min) with complete M199 media, which was replenished every other day. For coculturing with hMSC, the culture media was gradually replaced, during the first week, with complete α-MEM. One week after re-endothelialization ($t=8$ days), prestained hMSCs (red, Claret-CellVue®; Sigma-Aldrich) were seeded onto the same matrix by injection as detailed in the SM section 1.8. Seven days after MSCs were included in the coculture ($t=15$ days), human recombinant vascular endothelial growth factor (VEGF; Sigma-Aldrich) was added (3 ng/mL) and replenished every other day for an additional week. Online monitoring was conducted throughout these experiments, to assess cell viability, metabolism, process cytotoxicity, and maintenance of physiological pH. Cell viability was determined using dynamic AlamarBlue measurements on days 1, 6, 10, 15 and 21. Measurements of glucose (Freestyle™; Abbott Laboratories) and lactate (Lactate scout; EKF Diagnostics) were performed throughout the study. Cytotoxicity was evaluated in culture media 24 and 48 h after media replacement by measuring the activity of lactate dehydrogenase (LDH) using an LDH cytotoxicity detection kit (Roche), according to the manufacturer's instructions. LDH measurements represent the excess measured quantity after blank substitution (supplemented fresh culture media not exposed to cells kept for the same time duration within the same culture conditions). Background absorbance was eliminated by subtracting reads at 620 nm from the actual reads at 492 nm. Media pH was measured throughout the process using a standard narrow-electrode pH meter (Seven Easy™; Mettler Toledo) and maintained at physiological levels (7.2–7.4, data not shown) by changing the incubator's CO_2 concentration.

HUVEC-GFPs were live-imaged within the vascular network through the perfusion chamber glass cover on days 3, 10, and 21 using Olympus SZX16 (Olympus Corporation) binocular fluorescent microscope equipped with $0.8\times$ dry macro-lens with numerical aperture of 0.3 and a working distance of 81 mm. Exposure times were coordinated with those previously determined for blank matrices (before seeding, data not shown). On day 21 the matrices were removed from the bioreactor and subjected to fluorescent histological cross-section analyses (see SM section 1.8) imaged with LSM700 (Carl Zeiss).

Statistical analysis

A pilot screening experiment ($n=6$ biological replica per treatment group, Supplementary Fig. S2) was used to verify results' normal distribution and estimate sample size required based on 70% of measured effect size given conventional $\alpha=0.05$ and minimal power of 80%. Outliers were excluded based on the Mahalanobis D^2 method. Border zone cases were evaluated by the ''Jacknife'' criteria as well. For all experiments matrices were randomly allocated for each group. Unless otherwise specified, results are expressed as the mean ± standard deviation of either five or three biological repetitions per each experimental group in static ($n=5$) and dynamic ($n=3$) studies. Statistical significance in the differences of the means at individual time point experiments was evaluated by one-way analyses of variance (ANOVA) and Tukey's HSD test for multiple comparisons. Two-way ANOVA with Tukey's HSD *post hoc* correction for interaction and α-level adjustment for multiple comparisons was used to test the statistical significance of differences among groups through time. Particular contrast tests on individual treatment effect versus control based on least square mean estimates per group were performed to calculate the p-value. In all comparisons, $p<0.05$ was considered significant. Statistical analyses were done using JMP 6.0 statistical software (SAS™).

Results

Assessment of pcECM cell support and capacity

The specific binding of the collagen-binding peptides (CBPs) to the decellularized thick pcECM was similar to that observed with commercial collagen (Supplementary Fig. S3) thereby validating the pcECM structural integrity and suggesting that it may provide functional support for reseeded cells. Treating the pcECM with HA was shown to be more effective in increasing cell attachment and proliferation than treatments with RGD (Arg-Gly-Asp) containing collagen-binding peptides, cross-linking, nitrocellulose or sulfated glycosaminoglycans (GAGs, see SM section 1.1, Supplementary Results and Supplementary Fig. S2).

To measure the scaffold's cell-holding capacity, increasing densities of hMSCs ($n=5$ per seeding density) were seeded on untreated and HA-treated decellularized scaffolds, cultured under static conditions for 24 h, and analyzed by AlamarBlue, as detailed in the SM sections 1.2 and 1.3. The cell-loading capacity of HA-treated scaffolds (4.0×10^5 cells/cm^2) was significantly higher ($p<0.0001$) than that of the untreated scaffolds (2.7×10^5 cells/cm^2) (Fig. 2a), and demonstrated high correlation ($R^2>0.96$) between the modeled and empirically measured cell attachments (Fig. 2b). To characterize the effect of cell attachment on the proliferation and cell growth profile, hMSCs were seeded on untreated and HA-treated scaffolds in two densities, one below the maximal density of untreated scaffolds (Fig. 2c) and one above the maximal density of HA-treated scaffolds

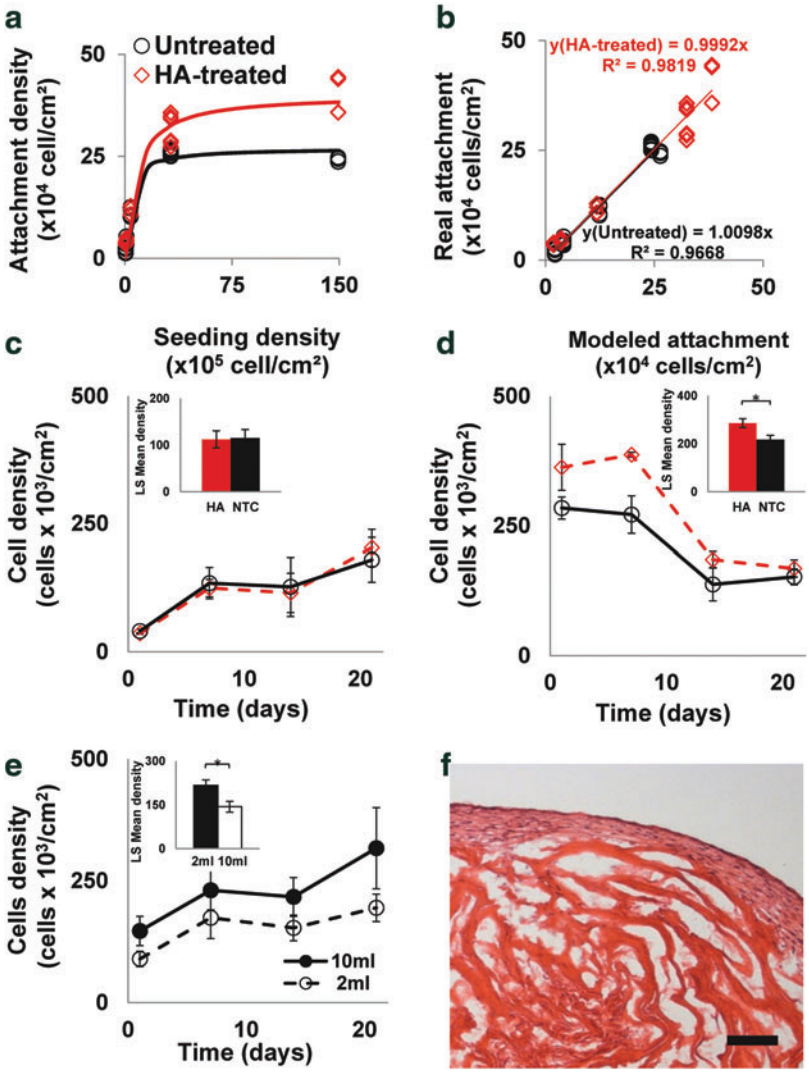

FIG. 2. Assessment of the pcECM scaffolds' maximal cell capacity. Mathematical modeling of empirical data sets **(a)** and a goodness of fit between predicted and measured values **(b)** for hyaluronic acid (HA) treated (*diamonds*) and nontreated (*circles*) pcECM matrices showing the attachment density as a function of initial seeding density. The cell loading capacity of HA-treated scaffolds (4.0×10^5 cells/cm^2) was significantly higher ($p<0.0001$) than that of the nontreated pcECM matrices (2.7×10^5 cells/cm^2). Cell density changes as a function of time for low **(c)** and high **(d)** seeding densities (5×10^4 and 1.5×10^7 cells/cm^2, respectively). The effect of medium volume on cell density is shown in **(e)**. Hematoxylin and eosin (H&E) staining of representative histological cross sections of reseeded pcECM constructs that were cultivated for 21 days, under static culture conditions **(f)**. For each experimental group and density there are five biological replicas ($n=5$). *Insets* in **(c, e)** show the least square means computed by two-way analyses of variance (ANOVA). * Denotes significantly different results $p<0.05$. Scale bar: **(f)**, 100 μm. pcECM, porcine cardiac ventricular extracellular matrix. Color images available online at www.liebertpub.com/tea

(Fig. 2d), and cultured for 21 days. While no significant difference was observed between the treated matrices and pcECM control at the low seeding density, the HA-treated scaffolds of the high seeding density, supported cell growth in significantly higher densities ($p<0.05$) throughout most of the culturing period (14 days), finally approaching densities similar to those measured on the untreated scaffolds ($1.8\pm0.3\times10^5$ cells/cm^2) after 21 days.

To assess the effect of the medium volume on the final density of the cultivated cells, hMSCs seeded on untreated scaffolds were cultured for 21 days in either 2 or 10 mL of excess culture media, showing higher final densities ($3.1\pm0.8\times10^5$ cells/cm^2, Fig. 2e) when excess volume was used corresponding to the predicted maximal cell capacity of the pcECM. Histological examination performed 21 days postseeding revealed that the cells were only able to penetrate 100 μm deep into the pcECM (Fig. 2f and Supplementary Fig. S4). However, their volumetric density—estimated by dividing the surface density with cellular penetration depth of 0.01 cm/100 μm—was high ($\sim2.7\times10^7$ cells/cm^3).

We also applied the same model for a different cell type, HUVECs, as an additional verification of the model sensitivity, revealing a pcECM maximal loading capacity for endothelial cells at a density of 5.4×10^4 cells/cm^2 (Supplementary Fig. S5a, b). The loading capacity for HUVECs was calculated to be fivefold less than that measured for hMSCs on the same scaffolds. This difference can be attributed to different penetration depths as the HUVEC appeared to remain at a monolayer coating of the pcECM surface rather than penetrate inside and remodel it (Supplementary Fig. S5c). These values for endothelial cells are also similar to the cell density of native porcine tissue coronary artery as evaluated through image analyses of confocal scans taken from within a freshly harvested porcine coronary artery ($5.0\pm0.7\times10^4$ cells/cm^2, Supplementary Fig. S5d).

Proving feasibility for pcECM support of cardiac cells

The relevancy of pcECM to cardiac tissue engineering was demonstrated by its support of hESC-CM (SM section 1.5) forming synchronously beating constructs just 3 days postseeding (Supplementary Movie SM1). Beating lasted for at least 3 more weeks during which time, histological cross sections revealed the presence of the hESC-CM, which were positively stained for Troponin I, serving as a marker of the cardiac muscle contraction machinery (Supplementary Fig. S6). In terms of maximal penetration depth,

hESC-CMs were localized in the initial 100 μm distance from the surface, similar to what was observed with hMSC under identical static culture conditions.

Compartmentalized recellularization

A custom-made perfusion bioreactor was designed and used (Fig. 3a) to study the ability of decellularized pcECM (Fig. 3b) to support compartmentalization of cell growth under dynamic culture conditions (Fig. 3). Simultaneous perfusion of two recellularized thick pcECM scaffolds revealed fully perfused constructs after 48 h that had regained their full dimensions (Fig. 3c, d). Incubating bulk reseeded hMSCs for one and a half hours, before perfusion, yielded significantly higher ($p<0.05$) retention of cell densities (average of $92\%\pm10\%$ of the seeded cell quantity) compared to cells that were allowed to attach for 24 h, as determined following a day of perfusion at two physiologically relevant flow rates (40 and 80 mL/min, Fig. 3f). Utilizing an attachment time of 1.5 h followed by 7 days of perfusion at 40 mL/min (to decrease possible shear damages), resulted in hMSC penetration of up to 400 μm deep into the pcECM bulk (Fig. 3e, evidenced by cross-sectional H&E staining). Elongated cell nuclei aligned along the pcECM fibers suggest that cells were not only physically entrapped within the scaffold but also attached and anchored to the pcECM in a more natural way.

A second set of experiments ($n=4$) was performed to evaluate the long-term cell support ability of the dynamic culture system. HMSCs were statically precultured on the patch endocardial surface for 30 days, during which cell density steady states were reached (as modeled in Fig. 2 and imaged through live confocal in Fig. 3j). The subsequent dynamic cultivation for 14 days led to a significant increase ($p<0.001$) in cell proliferation of almost fourfold compared to the steady state value achieved under static conditions (Fig. 3g). Concomitantly, cell penetration toward the feeding blood vessels increased up to 13-fold compared to statically cultivated cells (Figs. 2f and 3h, respectively). Immunofluorescent staining for CD44 (green, counterstained with DAPI—blue, Fig. 3i) identified the reseeded cells attached through their HA receptor to the ECM fibers (red, autofluorescence).

In another set of experiments, the applicability of this system to support the re-endothelialization of the pcECM vascular conduits was demonstrated. HUVECs stably expressing GFP appeared to form a ''cobble stone-like'' morphology, as assessed through confocal live imaging (Fig. 3k, 13 days postseeding and dynamic cultivation), achieving a monolayer coating of the vascular network lumen (Fig. 3l). Further immunofluorescent staining with CD31 performed on cross sections of dynamically re-endothelialized constructs confirmed the endothelial identity of the GFP-expressing cells and their retention as a monolayer without deviation to other compartments within the pcECM scaffold.

Ex vivo *assembly and functionality of the ECM vascular network*

The assembly and functionality of the vascular network were assessed using hMSCs and GFP-expressing HUVECs reseeded within different compartments of the pcECM (bulk injections and vasculature perfusion, respectively) and cocultured under dynamic conditions for 21 days. Online monitoring using indirect cellular viability and metabolism-based assays revealed cell proliferation that was correlated to both increasing quantities of lactate production and to a parallel decrease in free glucose within the circulating culture media (Fig. 4a, b, respectively). The addition of VEGF on day 14 substantially induced cell proliferation, which, a week later, reached a density of 3.0×10^7 ($\pm11\%$) cells per scaffold (Fig. 4a). Fluctuations in the measured concentrations from a baseline value to lower (glucose consumption) and higher (lactate production) levels are the natural result of culture media replenishing; however, the amplitudes of these fluctuations correspond to cell metabolism. The measured LDH levels were indicative of cell death in the early stages of cell seeding, revealing residual cell death in the matrix measured 3 days after HUVEC seeding and 2 days ($t=9\pm1$) after the hMSCs were added to the coculture. LDH levels stabilized with time to baseline levels, suggesting biocompatibility of the system that does not lead to any significant cytotoxic effect. The lactate levels measured exhibited physiological levels (2–8 mM, as per the lactate meter manufacturer instructions) throughout the entire experimental timeline.

The presence and organization of HUVEC-GFPs ($t=3$ and 21 days) was also monitored online by fluorescent microscopy (Fig. 4c–e). Endothelial cells demonstrated sprouting of new capillary-like vessels either through preexisting pathways (Fig. 4e) or through the *de novo ex vivo* angiogenic sprouting (Fig. 5d). Confocal imaging of cross sections revealed that cocultured cells were able to reach an overall thickness of 1.7 mm (Fig. 5a). New blood vessels sprouted in areas containing high hMSC concentrations on the outer walls of preexisting blood vessels (indicted by rectangles Fig. 5a). The nascent blood vessel-like structures were observed as an ''eruption'' of endothelial cells (green) accompanied by hMSCs (red, Fig. 5c, d).

Discussion

Functional vascular supply is one of the most crucial impediments determining the post-transplantational fate of recellularized myocardial tissue constructs. Several strategies were suggested to circumvent these limitations. The use of cocultures incorporating endothelial and pericyte-like cells, with or without parenchymal model cells, was shown to improve the prospects of statically cultivated constructs by enhancing vessel sprouting and connectivity to the host tissue, post-transplantation.[11–14] In another approach, dynamic cultivation *in vitro* of nonvascularized constructs, using forced medium perfusion, was shown to increase cellular penetration and survival beyond diffusion limitations up to ~600 μm from the surface.[28–30] This value probably represents the upper bound of this approach, due to a tradeoff between insufficient supply of too-low perfusion pressures and excessive shear stress jeopardizing cell viabilities when too-high pressures are employed. In both these strategies, the key hurdle to achieving ultimate human applicable sized grafts is the long lag-time required for functional angiogenesis to occur ($\sim$2–3 weeks postimplantation).

In recent years it is becoming clearer that ''functional vascularization'' is probably required to push the envelope of current tissue engineering technologies into cellularization of

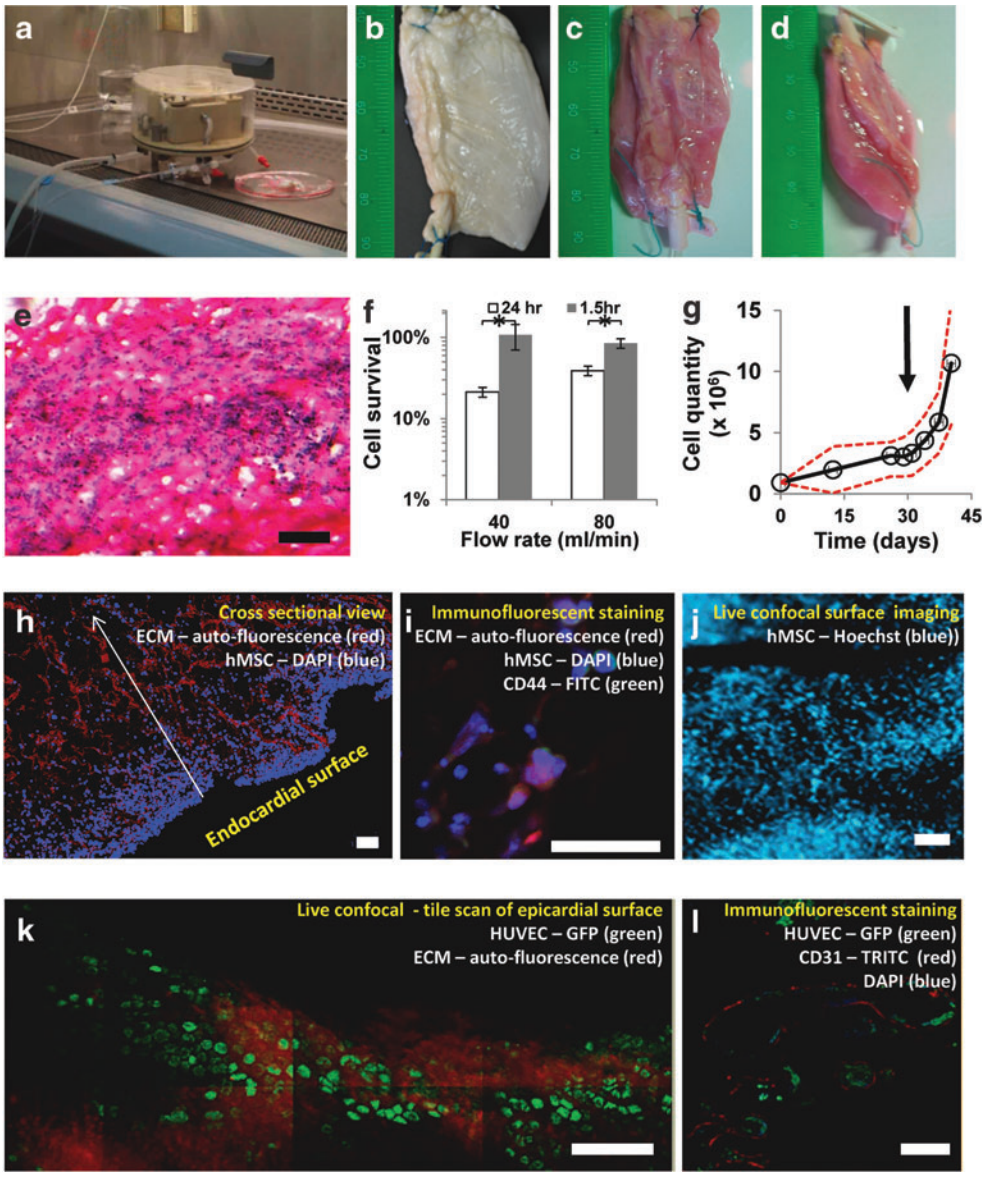

FIG. 3. Compartmentalized dynamic recellularization using monocultures of human mesenchymal stem cells (hMSCs) and human umbilical vein endothelial cells (HUVECs). A functioning perfusion chamber can be trans-located from the CO_2 incubator into a biological cabinet where sterile handling is available **(a)**. Using this system, decellularized thick pcECM scaffolds **(b)** regain full thickness appearance after 48 h of perfusion, as viewed from *top* or *side* **(c, d,** respectively). H&E staining 7 days postseeding **(e)**. Cell survival when cultivated under various physiological flow rates, using different seeding times (1.5 or 24 h), determined after 24 h of perfusion **(f)**. * Denotes significantly different results $p < 0.05$. Transferring of statically cultivated thick constructs ($t = 30$ days, marked with an *arrow*) to further cultivation in the dynamic system exhibits a significant ($p < 0.05$) increase in cell quantities **(g)**. *Dashed red line* represents the 95% confidence interval of the mean. H&E staining of histological cross-sections, 7 days postdynamic cultivation of hMSCs seeded through the bulk of the pcECM by injection—fibers are shown in *red* and cell nuclei in *blue* **(h)**. Specific antibody staining for CD44 suggests that the hMSCs are anchored to the pcECM through their HA receptors **(i)**. Live confocal imaging (hMSCs stained with Hoechst) of the endocardial surface after 21 days of static culture reveals densely populated surfaces in accordance with the mathematical model prediction of steady state densities **(j)**. Re-endothelialization of the vascular network within the pcECM is demonstrated using a monoculture of HUVEC-GFPs (*green*) forming 14 days postseeding and perfusion, a monolayer coating in a cobble stone-like formation **(k)**. Cross-section staining of the GFP expressing cells (*green*) with CD31 (*red*) demonstrated endothelium formation within the lumen of the blood vessel **(l)**. In all experiments, results represent three biological repetitions ($n = 3$). Scale bars: **(e)**, **(h)**, **(j–l)**, 100 μm; **(i)**, 50 μm. Color images available online at www.liebertpub.com/tea

thicker and physiologically more relevant constructs. This is particularly true when the implantation site is ischemic, for example, the infarcted heart. In this context, we define herein the concept of ''functional vascularization'' as the formation of a connectable branched vascular network within the construct that can be used to instantly supply the construct upon implantation. One approach to achieving such vascularization involves preimplantation of biomaterials either on the omentum[15] or around femoral arteriovenous loops employed as cardiac surgical flaps[31,32] with

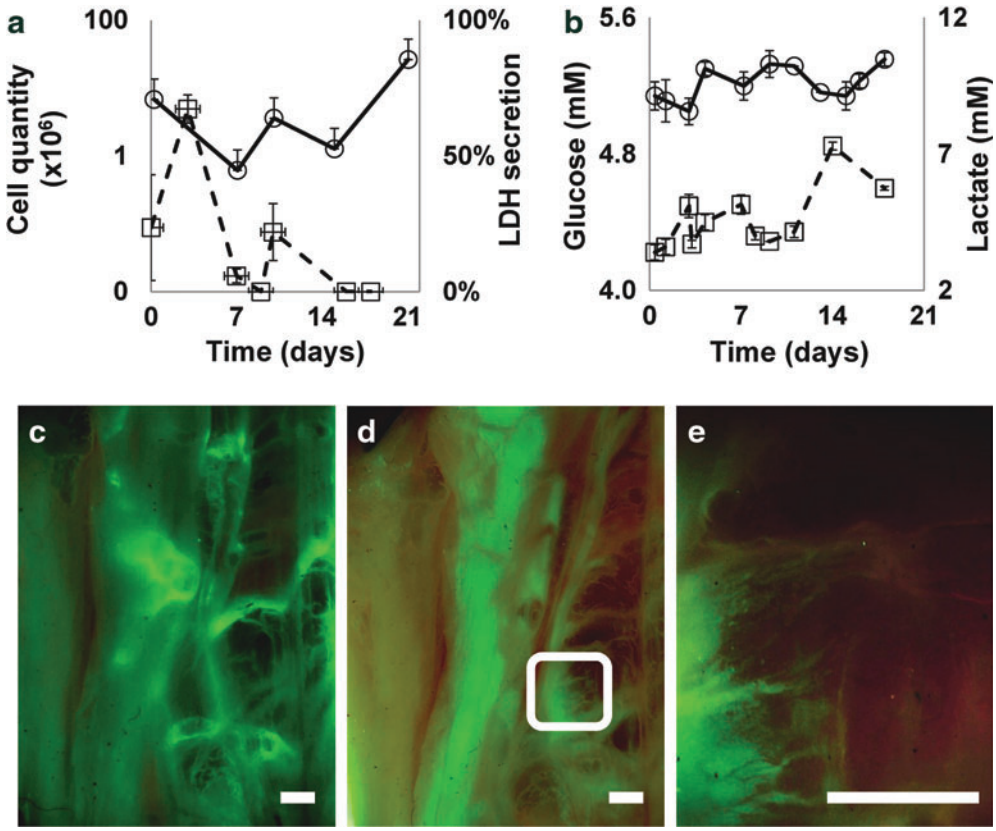

FIG. 4. Dynamic coculturing and revascularization of thick pcECM scaffolds. Online monitoring of cell culture conditions throughout the dynamic long-term cocultivation of HUVEC-GFPs and hMSCs **(a, b)**. Total cell quantity and cell lactate dehydrogenase (LDH)-cytotoxicity evaluation (*circles* and *squares*, respectively) are presented as a function of time **(a)**. Glucose consumption and lactate production (*circles* and *squares*, respectively) as measures of cell metabolism are presented as a function of time **(b)**. Reduction in glucose and increase in the level of lactate are attributed to cell metabolism whereas an increase in glucose and reduction in lactate levels are the consequences of culture medium changes zeroing the measurements to their baseline level. Vertical error bars represent standard error of the mean. Horizontal error bars represent standard deviation in time. Fluorescent monitoring of HUVEC-GFPs throughout the coculture dynamic experiment, showing live imaging of most of the large pcECM installed, including the main blood vessels at $t = 3$ **(c)**, and **(d)** 21 days. **(e)** A zoom-in view on the *white rectangle* appearing in **(d)**. Scale bars: 2 mm. In all experiments, results represent three biological repetitions ($n = 3$). Color images available online at www.liebertpub.com/tea

the aim of using the body as the ultimate supportive bioreactor. Another approach suggests the *ex vivo* construction of vascular beds from very basic building blocks using isolated native artery and vein embedded in a thymosin beta4-hydrogel.[4] The functionality of this vascular bed and the ultimate cellularized tissue thicknesses that can be obtained by this approach are still not sufficiently understood. Though producing valuable insights, both the above approaches are associated with donor site morbidity, further complicating clinical applicability.

An alternative approach to attaining functional construct vascularization may be premised on the use of preserved vascular conduits within decellularized myocardial ECM. Indeed, several groups including our own have recently reported on procedures for isolating myocardial ECM of porcine origin[7,18–23]—indicating the growing interest in this relatively new biomaterial. As the porcine heart is anatomically similar to the human heart,[7,23–25] this thick composite bio-material holds high potential for myocardial replacement therapies.[1,8,18,23] These scaffolds were also suggested to be advantageous over other materials given that they contain the ultra-structural mesh of inter-species conserved proteins and bioactive molecules that comprise natural myocardial ECM, which may better support expected regeneration and circumvent issues of immunogenicity. A distinction, however, should be made between whole heart porcine ECM templates[8,18,21] and downscaled ventricular full-wall ECM scaffolds.[7,23] Currently, the recellularization of big whole heart templates presents significant technological hurdles due to the complexity of cell types and quantities required,[8] their effective delivery and organization within organ distinct parenchymal localities,[33] and the development of relevant dynamic culturing technologies. The latter should enable continued viability and sterility for the relatively long time durations required for cell proliferation, organization, and maturation within their respective compartments. In this context the downscaling from whole heart templates to thick decellularized full wall ventricular slabs[7,23] may be advantageous, pending sufficient preservation of the ventricular wall major ECM constituents and a supportive blood vessel infrastructure. Thus, downscaling will likely substantially reduce the complexity of cell quantities, types and delivery

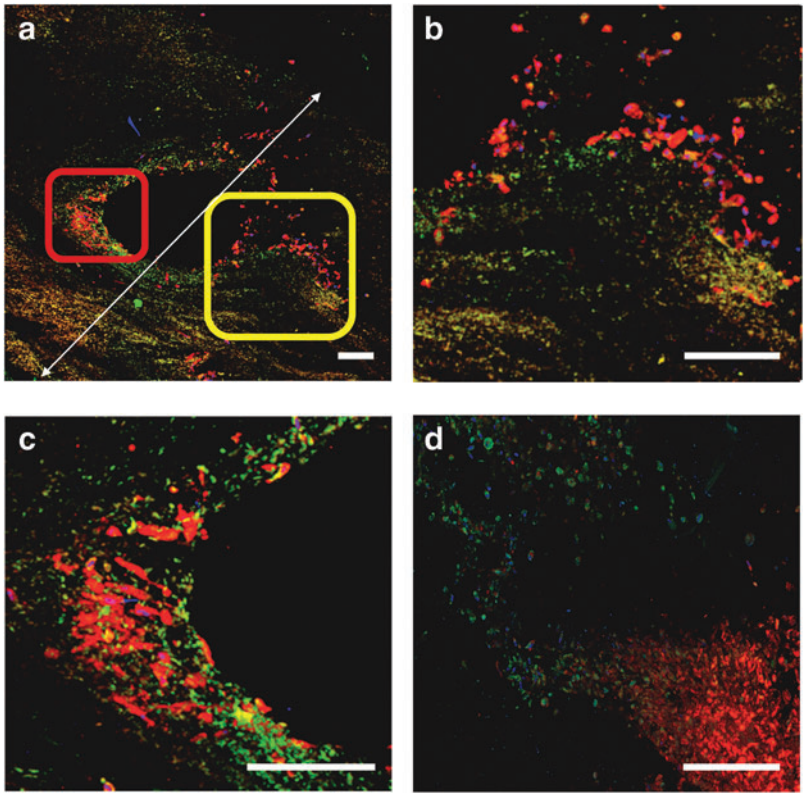

FIG. 5. *In vitro* functional angiogenesis. A cross-sectional overview of a small arteriole and its surrounding tissue 21 days post co-culture dynamic cultivation **(a,** 2×2 mm field of view). Sprouting of new vessel-like pathways, in various stages of maturation, is subjected to interplay between the sprouting HUVEC-GFPs (*green*) and hMSCs (CellVue® Claret, *red*) at the periphery of the supply arterioles. **(b, c)** Represent higher magnification of the rectangles marked in **(a;** *yellow* and *red*, respectively**)**. These *panels* show different stages of cell sprouting. At the initial stages of sprouting, hMSCs seem to concentrate around the base of the newly formed vessel **(c)**, followed by eruption of an endothelial cell front accompanied by fewer hMSCs as also demonstrated in **(b, d)**. Scale bars: 200 μm. In all experiments, results represent three biological repetitions ($n = 3$). Color images available online at www.liebertpub.com/tea

methods required for experimentation, and enable—under careful bioreactor design (Fig. 1)—more feasible long-term experimentation with compartmentalized recellularization in a noncontaminated environment.

In this study we aimed to reconstruct an inherent functional vascular bed that supports recellularization of physiologically relevant thicknesses using a completely *in vitro* setting (i.e., independent of donor organs or tissues). We hypothesized that the preserved vascular network within the pcECM scaffold studied herein can provide the basis for the *ex vivo* construction of thick (i.e., >600 mm) recellularized myocardial-like tissue constructs, in a compartmentalized manner. For these purposes thick pcECM was evaluated herein in terms of its cell support capacity and functional vasculature assembly under static and dynamic culture conditions, using a bioreactor system custom-built to provide physiological mimicking conditions *ex vivo*. Two cell types were primarily employed in this study and used as model cells for endothelial (HUVECs) and pericytic/parenchymal (MSCs) functions to enable possible self-assembly of more mature and functional blood vessels within the construct. The technology developed herein may be readily applicable to many other ECM-based approaches, regardless of the ECM tissue origin or parenchymal cell types required for the engineered construct ultimate function, so long as the inherent vascular network is preserved within the material.

The cell supporting capacity of pcECM scaffolds was initially evaluated under static culture conditions. We developed a simple methodology to mathematically model the maximal cell holding capacity of the pcECM (Fig. 2). The predicted (model) and measured (empirical data) maximal pcECM volumetric cell holding capacity (2.7×10^7 cells/cm^3) closely approximated the actual density of CM in the adult human heart (2×10^7 CM/cm^3).[34] Our suggested model was further validated in three ways. First, by artificially increasing the quantity of cell adhesion sites, a corresponding increase in the model's prediction of maximal cell capacity was revealed. Second, long-term cultivation exhibited convergence of cell densities even when the initial seeding densities were far below and above the model's estimated predictions. Third, when a different cell type was used (HUVECS) different values were obtained suggesting sensitivity of the model to specific cell–scaffold interactions (Supplementary Fig. S5). Interestingly, the values measured and computed for HUVECs also corresponded to the measured endothelial cell density in the luminal surface of the porcine coronary artery (SM section 1.4 and Supplementary Fig. S5d) and corresponded to that reported for completely biological engineered vascular grafts using human endothelial cells.[35]

Several other mathematical models have been suggested in recent years to enable the characterization of cell quantities within scaffold biomaterials under both static[36–40] and dynamic[29,41–45] culture conditions. In general, the models based on static cultivation are usually too complex to be routinely used for biological screening or biomaterial characterizing, while the dynamic models are usually multifactorial, limiting applicability when simple static conditions are at hand. To the best of our knowledge, this is the first time such a simple and easily applicable model is suggested for these purposes and could probably be easily applied to any particular cell and biomaterial scaffold combination within 24–96 h of seeding. Furthermore, our findings indicate that maximal cell capacity is an important cell–scaffold characteristic, which may predict the scaffold's long-term cell support ability given a set of defined culture conditions. Nevertheless, this

may be limited in applicability for scaffolds in which degradation is fast. For example, rapidly degrading scaffolds (e.g., PLGA) may modify their available surface area and diffusion patterns through time, affecting the cell maximal holding capacity of the scaffold. In our hands, though, the pcECM was only mildly remodeled during the experimental timeline and therefore our findings remained valid for at least 2–3 weeks—a period of time, which is usually applicable for most of the practical laboratory tests.

As the pcECM scaffold was isolated using decellularization, some damage may be expected, which usually comprises both GAG washout and the disruption of the collagenous structural network.[46,47] GAG and collagen-binding sites were previously reported to independently influence cell adhesion and proliferation within the heart.[48] Therefore, we performed screening experiments in which cell adhesion sites were artificially introduced into the pcECM, with the aim of identifying the optimal cell adhesion site modification for model verification. These screening experiments may also indicate the extent of the damage that might have been caused by the decellularization, given that the addition of a missing component would be expected to result in increased cell attachment and proliferation on the pcECM. Thus, CBPs, GAG (representatives of both sulfated and nonsulfated groups), nitrocellulose, and simple cross-linking were evaluated with various combinations (Supplementary Figs S2 and S3). The functional collagen binding with specific CBP-RGD residues suggested the preservation of collagen-binding sites during our decellularization procedure. Furthermore, the fact that no significant difference was observed between pcECM treated with CBP containing RGD moieties compared to nontreated matrices in terms of cell attachment and proliferation suggests that structural binding motifs are not lacking within the pcECM. In contrast, addition of glycoside moieties (nitrocellulose, sulfated and nonsulfated GAG) were shown to be much better cell adhesion modifiers (with the best effect measured for HA addition, $p = 1.8 \times 10^{-6}$) postdecellularization. Interestingly, though initially differing, the final cell density ($t = 21$) was similar in both HA-conjugated and nontreated pcECM matrices, suggesting that the effect of GAG conjugation is limited. This transient effect might be attributable to the synthesis and secretion of GAG by the reseeded cells themselves,[49] altering the pcECM composition with time.

To better visualize the cells within the reseeded pcECM scaffolds, histological sections were performed, revealing a relatively high cell density within a narrow depth of penetration ($\sim 100\,\mu m$). This limited penetration depth is similar to the known ''soft-tissue'' diffusion limitation that is associated with heart and muscle regeneration,[1,4–6] further suggesting that the pcECM scaffolds can be recellularized to a physiologically similar density. Interestingly, the cultivation of cardiac parenchymal cells (i.e., CM) resulted in the formation of synchronously beating constructs starting from 3 days postseeding (Supplementary Movie SM1 and Supplementary Data). In fact, the CMs were well supported by the pcECM within a similar penetration depth as that measured for hMSCs (Supplementary Fig. S6).

We therefore hypothesized that nutrient and medium volume may be a limiting factor in cell proliferation within these initial $100\,\mu m$ of penetration depth. Increasing the volume of culture media per construct by fivefold enabled us to reach the predicted theoretical values, for hMSCs used here as model cells, after 21 days of culture. However, no further improvements were observed, even when using larger medium volumes (data not shown), pointing to the limitation associated with static culture conditions. This observation led us to the development of the dynamic cultivation platform for thick pcECM constructs presented herein.

To enable long-term support of cellular proliferation we designed a new perfusion bioreactor system, encompassing physiological mimicking pulsatile perfusion capabilities along with room for future electro-mechanical stimulation subsystems. We hypothesized that by using the perfusion features of this bioreactor, we can provide cell support within a relatively thick and viable construct, which relies on the pcECM's inherently preserved blood vessel infrastructure. To test its applicability, we initially conducted a series of short-term optimizations to ensure proper physiological flow rates and sufficient seeding times were used. These experiments revealed that when hMSCs were injected into the bulk cavities of the thick pcECM scaffold and allowed to adhere for 90 min, high cell viabilities are achieved over 48 h periods, with reseeded and perfused constructs swelling back to human equivalent left ventricular dimensions. The cultivation of such constructs for 7 days revealed cell clusters aligned to the ECM fibers within the scaffold bulk, with a depth of up to four times greater than that observed under static culture conditions. Furthermore, the advantage of this bioreactor system over static tissue culture was demonstrated by sequential cultivation of statically precultured constructs that were allowed to reach cell density steady state, before their dynamic expansion for an additional period of 14 days. Under dynamic conditions, the observed increase in cell penetration and viability beyond the steady state values suggests that reseeded cells have migrated toward the nourishing blood vessels where presumably fresh oxygen and nutrients are available. The advantage of such an approach is in providing a biomimetic milieu for functional cell assembly that may, in turn, lead to CM orientation and survival, as also recently proposed by Chiu et al.[4]

Another major hurdle to any future transplantation strategy is achieving a proper vascular re-endothelialization of decellularized grafts, thus minimizing blood coagulation and aneurism formation.[50] The re-endothelialization is also a prerequisite to the support of thick tissue-engineered constructs. As a proof of concept, the isolated thick pcECM scaffold and its adapted bioreactor system were also studied in terms of their ability to support such re-endothelialization. Seeing as both the coculture with MSC[51,52] and the administration of VEGF[4,53] were previously reported to be associated with blood vessel sprouting and maturation, they were both used in our experimental setup. Under dynamic coculture conditions, the blood vessel network of the thick pcECM constructs became revitalized, exhibiting various levels of vessel sprouting and maturation. MSCs added to the culture system demonstrated a pericytic-like support for the endothelial cells as evident by the histological cross-section analyses performed, and further supported by several reports on the role of MSCs as pericytes *in vivo*.[54,55] The addition of VEGF to the culture media contributed to a dramatic increase in cell proliferation accompanied with vessel sprouting from various locations both through predetermined paths within the ECM and through *de novo* created tracks (Figs. 4

and 5 and Supplementary Fig. S7). The effect of VEGF addition to vessel sprouting was also recently reported by the Radisic group in a hydrogel model utilizing native arteries and veins as the main supplying vessels.[4] Of note is that, in our hands, the effect of VEGF addition was time dependent as its addition in premature states (i.e., before MSC seeding) resulted in insignificant re-endothelialization (data not shown). This is, to the best of our knowledge, the first time such a delicate process of vessel sprouting from within large reseeded acellular conduits (<1 mm in diameter, ~ 5–6 mm in length) has been documented in a completely *in vitro* environment. Thus, the bioreactor and scaffold setup presented in our work can also be used for further studies of the delicate interplay between various cell types related to angiogenesis and cardiac restoration therapies.

Finally, the coculture of endothelial cells and MSCs using this novel perfusion bioreactor system also enabled the achievement of a relatively thick cell-supportive ECM tissue construct (~ 1.7 mm, Fig. 5), which is, to the best of our knowledge, unprecedented in a completely *in vitro* system. This is comparable to the maximal reported thickness achieved to date using *in vivo* corporal systems as the optimal bioreactor setup.[31] Though the bioreactor design also contains additional means to provide both electrical and mechanical stimuli for preconditioning to improve cell organization within the scaffold these were not tested within the context of this article. Further experimentations are being conducted to address these issues.

In conclusion, this study presents two major findings/methodologies: The *ex vivo* genesis of *functional* vasculature and the quick characterization of scaffold biomaterials in terms of their maximal cell capacity and long-term cell support ability. Both methodologies reported herein were demonstrated through the use of pcECM thick constructs and a new custom-developed dynamic cultivation technology. We have shown that using such a careful and systematic approach, the support of physiological-like cell densities in up to 1.7 mm thick viable constructs is possible in a completely *ex vivo* environment. These findings raise the bar for state-of-the-art myocardial tissue engineering and reaffirm the potential of thick acellular pcECM as an exciting biomaterial with a clinical potential for regenerative cardiac medicine. Furthermore, this system offers a unique platform for *in vitro* studies of decellularized soft-tissue ECM-based tissue engineering strategies, such as the pcECM demonstrated herein. Nevertheless, to achieve morphologies that better resemble the cardiac native tissue, the incorporation of parenchymal cells (e.g., CM) into the dynamically cultivated constructs and the study of additional mechano-electrical stimulation in the designed bioreactor, are required. We expect such experimentation, to further exploit the potential of the thick pcECM matrix and bioreactor system reported herein.

Acknowledgments

This research was supported by the Israeli Science Foundation (grant No. 1563/10), the Singapore National Research Foundation under the CREATE program: The Regenerative Medicine Initiative in Cardiac Restoration Therapy Research, and the Randy L. and Melvin R. Berlin Family Research Center for Regenerative Medicine. The authors would like to acknowledge the support of the following persons: Mr. Friedbert Gellerman from the Institute of Technical Chemistry (Leibniz University of Hanover) for his hard and professional work in accurately producing the reported bioreactor according to our demanding designs, making it a working reality; Dr. Maayan Duvshani Eshet (Technion, LS&E infrastructure unit) for her help in providing proper imaging guidance and equipment; Prof. Gera Neufeld (Technion, Faculty of Medicine) for the contribution of the GFP-expressing HUVECs; and the Advanced Molecular Pathology Laboratory (AMPL) of the Institute of Molecular and Cell Biology (IMCB) of the Agency for Science Technology and Research (A*Star) for their histopathological support with hES-CM histology.

Disclosure statement

No competing financial interests exist.

References

1. Sarig, U., and Machluf, M. Engineering cell platforms for myocardial regeneration. Expert Opin Biol Ther **11,** 1055, 2011.
2. Soler-Botija, C., Bago, J.R., and Bayes-Genis, A. A bird's-eye view of cell therapy and tissue engineering for cardiac regeneration. Ann N Y Acad Sci **1254,** 57, 2012.
3. Karam, J.P., Muscari, C., and Montero-Menei, C.N. Combining adult stem cells and polymeric devices for tissue engineering in infarcted myocardium. Biomaterials **33,** 5683, 2012.
4. Chiu, L.L., Montgomery, M., Liang, Y., Liu, H., and Radisic, M. Perfusable branching microvessel bed for vascularization of engineered tissues. Proc Natl Acad Sci U S A **109,** E3414, 2012.
5. Kaully, T., Kaufman-Francis, K., Lesman, A., and Levenberg, S. Vascularization—the conduit to viable engineered tissues. Tissue Eng Part B Rev **15,** 159, 2009.
6. Ko, H.C., Milthorpe, B.K., and McFarland, C.D. Engineering thick tissues—the vascularisation problem. Eur Cell Mater **14,** 1, 2007.
7. Sarig, U., Au-Yeung, G.C., Wang, Y., Bronshtein, T., Dahan, N., Boey, F.Y., Venkatraman, S.S., and Machluf, M. Thick acellular heart extracellular matrix with inherent vasculature: a potential platform for myocardial tissue regeneration. Tissue Eng Part A **18,** 2125, 2012.
8. Badylak, S.F., Taylor, D., and Uygun, K. Whole-organ tissue engineering: decellularization and recellularization of three-dimensional matrix scaffolds. Annu Rev Biomed Eng **13,** 27, 2011.
9. Bronshtein, T., Au-Yeung, G.C., Sarig, U., Nguyen, E.B., Mhaisalkar, P.S., Boey, Y.C., Subbu, V.S., and Machluf, M. A mathematical model for analyzing the elasticity, viscosity and failure of soft tissue: comparison of native and decellularized porcine cardiac extracellular matrix for tissue engineering. Tissue Eng Part C Methods **19,** 620, 2013.
10. Radisic, M., Marsano, A., Maidhof, R., Wang, Y., and Vunjak-Novakovic, G. Cardiac tissue engineering using perfusion bioreactor systems. Nat Protoc **3,** 719, 2008.
11. Caspi, O., Lesman, A., Basevitch, Y., Gepstein, A., Arbel, G., Habib, I.H., Gepstein, L., and Levenberg, S. Tissue engineering of vascularized cardiac muscle from human embryonic stem cells. Circ Res **100,** 263, 2007.
12. Lesman, A., Habib, M., Caspi, O., Gepstein, A., Arbel, G., Levenberg, S., and Gepstein, L. Transplantation of a tissue-

engineered human vascularized cardiac muscle. Tissue Eng Part A **16,** 115, 2009.
13. Iyer, R.K., Chiu, L.L., and Radisic, M. Microfabricated poly(ethylene glycol) templates enable rapid screening of triculture conditions for cardiac tissue engineering. J Biomed Mater Res A **89,** 616, 2009.
14. Sekine, H., Shimizu, T., Hobo, K., Sekiya, S., Yang, J., Yamato, M., Kurosawa, H., Kobayashi, E., and Okano, T. Endothelial cell coculture within tissue-engineered cardiomyocyte sheets enhances neovascularization and improves cardiac function of ischemic hearts. Circulation **118,** S145, 2008.
15. Dvir, T., Kedem, A., Ruvinov, E., Levy, O., Freeman, I., Landa, N., Holbova, R., Feinberg, M.S., Dror, S., Etzion, Y., Leor, J., and Cohen, S. Prevascularization of cardiac patch on the omentum improves its therapeutic outcome. Proc Natl Acad Sci U S A **106,** 14990, 2009.
16. Ott, H.C., Matthiesen, T.S., Goh, S.K., Black, L.D., Kren, S.M., Netoff, T.I., and Taylor, D.A. Perfusion-decellularized matrix: using nature's platform to engineer a bioartificial heart. Nat Med **14,** 213, 2008.
17. Akhyari, P., Aubin, H., Gwanmesia, P., Barth, M., Hoffmann, S., Huelsmann, J., Preuss, K.H., and Lichtenberg, A. The quest for an optimized protocol for whole heart decellularization: a comparison of three popular and a novel decellularization technique and their diverse effects on crucial extracellular matrix qualities. Tissue Eng Part C Methods **17,** 915, 2011.
18. Wainwright, J.M., Czajka, C.A., Patel, U.B., Freytes, D.O., Tobita, K., Gilbert, T.W., and Badylak, S.F. Preparation of cardiac extracellular matrix from an intact porcine heart. Tissue Eng Part C Methods **16,** 525, 2010.
19. Wang, B., Borazjani, A., Tahai, M., Curry, A.L., Simionescu, D.T., Guan, J., To, F., Elder, S.H., and Liao, J. Fabrication of cardiac patch with decellularized porcine myocardial scaffold and bone marrow mononuclear cells. J Biomed Mater Res A **94,** 1100, 2010.
20. Eitan, Y., Sarig, U., Dahan, N., and Machluf, M. Acellular cardiac extracellular matrix as a scaffold for tissue engineering: in vitro cell support, remodeling, and biocompatibility. Tissue Eng Part C Methods **16,** 671, 2010.
21. Weymann, A., Loganathan, S., Takahashi, H., Schies, C., Claus, B., Hirschberg, K., Soos, P., Korkmaz, S., Schmack, B., Karck, M., and Szabo, G. Development and evaluation of a perfusion decellularization porcine heart model—generation of 3-dimensional myocardial neoscaffolds. Circ J **75,** 852, 2011.
22. Singelyn, J.M., DeQuach, J.A., Seif-Naraghi, S.B., Littlefield, R.B., Schup-Magoffin, P.J., and Christman, K.L. Naturally derived myocardial matrix as an injectable scaffold for cardiac tissue engineering. Biomaterials **30,** 5409, 2009.
23. Schulte, J.B., Simionescu, A., and Simionescu, D.T. The acellular myocardial flap; a novel extracellular matrix scaffold enriched with patent microvascular networks and biocompatible cell niches. Tissue Eng Part C Methods **19,** 518, 2013.
24. Hughes, H.C. Swine in cardiovascular research. Lab Anim Sci **36,** 348, 1986.
25. Heusch, G., Skyschally, A., and Schulz, R. The in-situ pig heart with regional ischemia/reperfusion—ready for translation. J Mol Cell Cardiol **50,** 951, 2011.
26. Varshavsky, A., Kessler, O., Abramovitch, S., Kigel, B., Zaffryar, S., Akiri, G., and Neufeld, G. Semaphorin-3B is an angiogenesis inhibitor that is inactivated by furin-like pro-protein convertases. Cancer Res **68,** 6922, 2008.
27. Wang, Y., Bronshtein, T., Sarig, U., Boey, F.Y.C., Venkatraman, S.S., and Machluf, M. Endothelialization of acellular porcine ECM with chemical modification. Int J Biosci Biochem Bioinforma **2,** 363, 2012.
28. Radisic, M., Yang, L., Boublik, J., Cohen, R.J., Langer, R., Freed, L.E., and Vunjak-Novakovic, G. Medium perfusion enables engineering of compact and contractile cardiac tissue. Am J Physiol Heart Circ Physiol **286,** H507, 2004.
29. Dvir, T., Benishti, N., Shachar, M., and Cohen, S. A novel perfusion bioreactor providing a homogenous milieu for tissue regeneration. Tissue Eng **12,** 2843, 2006.
30. Radisic, M., Malda, J., Epping, E., Geng, W., Langer, R., and Vunjak-Novakovic, G. Oxygen gradients correlate with cell density and cell viability in engineered cardiac tissue. Biotechnol Bioeng **93,** 332, 2006.
31. Lim, S.Y., Hsiao, S.T., Lokmic, Z., Sivakumaran, P., Dusting, G.J., and Dilley, R.J. Ischemic preconditioning promotes intrinsic vascularization and enhances survival of implanted cells in an in vivo tissue engineering model. Tissue Eng Part A **18,** 2210, 2012.
32. Tee, R., Morrison, W.A., Dusting, G.J., Liu, G.S., Choi, Y.S., Hsiao, S.T., and Dilley, R.J. Transplantation of engineered cardiac muscle flaps in syngeneic rats. Tissue Eng Part A **18,** 1992, 2012.
33. Soto-Gutierrez, A., Wertheim, J.A., Ott, H.C., and Gilbert, T.W. Perspectives on whole-organ assembly: moving toward transplantation on demand. J Clin Invest **122,** 3817, 2012.
34. Madden, L.R., Mortisen, D.J., Sussman, E.M., Dupras, S.K., Fugate, J.A., Cuy, J.L., Hauch, K.D., Laflamme, M.A., Murry, C.E., and Ratner, B.D. Proangiogenic scaffolds as functional templates for cardiac tissue engineering. Proc Natl Acad Sci U S A **107,** 15211, 2010.
35. L'Heureux, N., Paquet, S., Labbe, R., Germain, L., and Auger, F.A. A completely biological tissue-engineered human blood vessel. FASEB J **12,** 47, 1998.
36. Dunn, J.C., Chan, W.Y., Cristini, V., Kim, J.S., Lowengrub, J., Singh, S., and Wu, B.M. Analysis of cell growth in three-dimensional scaffolds. Tissue Eng **12,** 705, 2006.
37. Jeong, D., Yun, A., and Kim, J. Mathematical model and numerical simulation of the cell growth in scaffolds. Biomech Model Mechanobiol **11,** 677, 2012.
38. Carlier, A., Chai, Y.C., Moesen, M., Theys, T., Schrooten, J., Van Oosterwyck, H., and Geris, L. Designing optimal calcium phosphate scaffold-cell combinations using an integrative model-based approach. Acta Biomater **7,** 3573, 2011.
39. Catt, C., Schuurman, W., Sengers, B., van Weeren, P., Dhert, W., Please, C., and Malda, J. Mathematical modelling of tissue formation in chondrocyte filter cultures. Eur Cells Mater **22,** 377, 2011.
40. Gerisch, A., Painter, K., Chauvière, A., Preziosi, L., and Claude, V. Mathematical modeling of cell adhesion and its applications to developmental biology and cancer invasion. In: Chauvière, A., Preziosi, L., and Claude, V., eds. Cell Mechanics: From Single Scale-Based Models to Multiscale Modeling. Boca Raton, FL: CRC Press, 2010, pp. 313–341.
41. Causin, P., and Sacco, R. A computational model for biomass growth simulation in tissue engineering. Commun Appl Ind Math **2,** 370, 2011. DOI: 10.1685/journal.caim.370.
42. Olivares, A.L., and Lacroix, D. Simulation of cell seeding within a three-dimensional porous scaffold: a fluid-particle analysis. Tissue Eng Part C Methods **18,** 624, 2012.
43. Coletti, F., Macchietto, S., and Elvassore, N. Mathematical modeling of three-dimensional cell cultures in perfusion bioreactors. Ind Eng Chem Res **45,** 8158, 2006.

44. Sanz-Herrera, J., García-Aznar, J., and Doblaré, M. A mathematical approach to bone tissue engineering. Philos Trans A Math Phys Eng Sci **367,** 2055, 2009.
45. Shakeel, M., Matthews, P.C., Graham, R.S., and Waters, S.L. A continuum model of cell proliferation and nutrient transport in a perfusion bioreactor. Math Med Biol **30,** 21, 2013.
46. Gilbert, T.W., Sellaro, T.L., and Badylak, S.F. Decellularization of tissues and organs. Biomaterials **27,** 3675, 2006.
47. Crapo, P.M., Gilbert, T.W., and Badylak, S.F. An overview of tissue and whole organ decellularization processes. Biomaterials **32,** 3233, 2011.
48. Michel, J.B. Anoikis in the cardiovascular system: known and unknown extracellular mediators. Arterioscler Thromb Vasc Biol **23,** 2146, 2003.
49. Gandhi, N.S., and Mancera, R.L. The structure of glycosaminoglycans and their interactions with proteins. Chem Biol Drug Des **72,** 455, 2008.
50. Dahan, N., Zarbiv, G., Sarig, U., Karram, T., Hoffman, A., and Machluf, M. Porcine small diameter arterial extracellular matrix supports endothelium formation and media remodeling forming a promising vascular engineered biograft. Tissue Eng Part A **18,** 411, 2012.
51. Duffy, G.P., Ahsan, T., O'Brien, T., Barry, F., and Nerem, R.M. Bone marrow-derived mesenchymal stem cells promote angiogenic processes in a time- and dose-dependent manner in vitro. Tissue Eng Part A **15,** 2459, 2009.
52. Wang, Y., Bronshtein, T., Sarig, U., Nguyen, E.B., Boey, Y.C., Subbu, V.S., and Machluf, M. A mathematical model predicting the co-culture dynamics of endothelial and mesenchymal stem cells for tissue regeneration. Tissue Engineering Part A **19,** 1155, 2013.
53. Chiu, L.L., Radisic, M., and Vunjak-Novakovic, G. Bioactive scaffolds for engineering vascularized cardiac tissues. Macromol Biosci **10,** 1286, 2010.
54. Caplan, A.I. All MSCs are pericytes? Cell Stem Cell **3,** 229, 2008.
55. da Silva Meirelles, L., Caplan, A.I., and Nardi, N.B. In search of the in vivo identity of mesenchymal stem cells. Stem Cells **26,** 2287, 2008.

Address correspondence to:
Marcelle Machluf, PhD
The Laboratory of Cancer Drug Delivery
& Mammalian Cell Technology
Faculty of Biotechnology and Food Engineering
Technion–Israel Institute of Technology
Haifa 32000
Israel

E-mail: machlufm@tx.technion.ac.il

Received: August 7, 2014
Accepted: January 7, 2015
Online Publication Date: March 17, 2015